ORGANIC LETTERS

2013
Vol. 15, No. 22
5714–5717

Ladder-Type BN-Embedded Heteroacenes with Blue Emission

Xinyang Wang,[†] Fan Zhang,*[,†] Jun Liu,[‡] Ruizhi Tang,[†] Yubin Fu,[†] Dongqing Wu,[†] Qing Xu,[†] Xiaodong Zhuang,[†] Gufeng He,[‡] and Xinliang Feng*[,†,§]

School of Chemistry and Chemical Engineering and Department of Electronic Engineering, Shanghai Jiao Tong University, Shanghai 200240, P. R. China, and Max-Planck Institute for Polymer Research, Ackermannweg 10, 55128 Mainz, Germany

fan-zhang@sjtu.edu.cn; feng@mpip-mainz.mpg.de

Received September 23, 2013

ABSTRACT

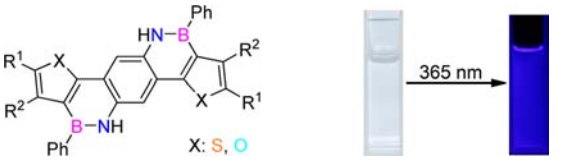

Using a concise synthetic strategy, a series of novel ladder-type BN-embedded heteroacenes were successfully synthesized. Their molecular skeletons render the versatile modification which is desirable for achieving unique physical properties. Organic light-emitting diode devices based on BN-embedded heteroacenes were subsequently fabricated, demonstrating their promising application as blue emitters.

Owing to their outstanding electronic properties, acenes are among the most promising organic semiconductors for application in electronic devices such as organic field-effect transistors (OFETs) and organic light-emitting diodes (OLEDs).[1] In particular, ladder-type acenes that feature rigid planar backbones and extended π-conjugation exhibit high charge-carrier mobility, intense luminescence, and unique self-assembly behavior in solution and on the surface.[2] Incorporation of heteroatoms into ladder-type acene backbones represents an efficient strategy for fine-tuning the solid-state packing and optoelectronic properties of the molecules and can significantly improve the environmental stability of the materials.[3] For example, dithienyl[*a*,*h*]anthracene (**II**) exhibits a significantly different crystal packing from its all-carbon analog dibenz[*a*,*h*]-anthracene (**I**), which most likely arises from the induced S−S intermolecular interactions (Figure 1).

A large number of ladder-type heteroacenes that contain different heteroatoms, such as N, S, Si, P, and B, have been explored extensively during the past decade.[5] Among these, heteroacenes with more than five fused aromatic rings remain the challenging synthetic targets and are worthwhile exploring as models for heteroatom-doped graphene[6] and graphene nanoribbon, as well as for molecular wire.[7] Replacing a C=C moiety with an isoelectronic

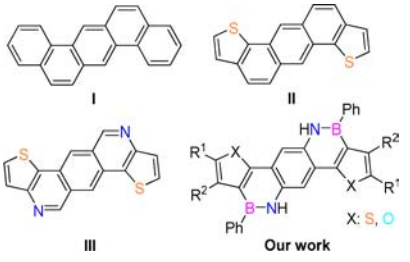

Figure 1. Typical ladder-type acenes.[4]

[†] School of Chemistry and Chemical Engineering, Shanghai Jiao Tong University.
[‡] Department of Electronic Engineering, Shanghai Jiao Tong University.
[§] Max-Planck Institute for Polymer Research.

(1) (a) Anthony, J. E. *Chem. Rev.* **2006**, *106*, 5028. (b) Anthony, J. E. *Angew. Chem., Int. Edit* **2008**, *47*, 452.
(2) Araneda, J. F.; Neue, B.; Piers, W. E.; Parvez, M. *Angew. Chem., Int. Edit.* **2012**, *51*, 8546.
(3) Yamamoto, T.; Takimiya, K. *J. Am. Chem. Soc.* **2007**, *129*, 2224.
(4) (a) Zhang, Q. T.; Tour, J. M. *J. Am. Chem. Soc.* **1997**, *119*, 9624. (b) Pietrangelo, A.; MacLachlan, M. J.; Wolf, M. O.; Patrick, B. O. *Org. Lett.* **2007**, *9*, 3571. (c) Pietrangelo, A.; Patrick, B. O.; MacLachlan, M. J.; Wolf, M. O. *J. Org. Chem.* **2009**, *74*, 4918. (d) Osaka, I.; Shinamura, S.; Abe, T.; Takimiya, K. *J. Mater. Chem. C.* **2013**, *1*, 1297.
(5) Fukazawa, A.; Yamada, H.; Yamaguchi, S. *Angew. Chem., Int. Edit.* **2008**, *47*, 5582.
(6) Dou, C.; Saito, S.; Matsuo, K.; Hisaki, I.; Yamaguchi, S. *Angew. Chem., Int. Ed.* **2012**, *51*, 12206.

10.1021/ol402745r
Published on Web 10/24/2013

B−N fragment to build up a BN-embedded heteroacene manifests some expected similarities in geometric structure but substantially different electronic features with respect to their all-carbon analogues.[8] Apparently, the different electronegativities between boron and nitrogen elements in the B−N unit play a critical role in tuning the molecular frontier orbitals and intermolecular interactions of heteroacenes.[9] Nevertheless, there are only few reports on BN-embedded heteroacenes,[10] and to date, no ladder-type example has been reported.

In this paper, we present a concise synthetic strategy based on highly efficient cyclization of nitrogen-directed aromatic borylation for the synthesis of a series of novel ladder-type BN-embedded heteroacenes (**1**−**3**). The geometric and electronic structures of these heteroacenes were investigated systematically by X-ray crystallography, optical spectroscopy, and cyclic voltammetry. Furthermore, the preliminary OLED-device fabrication based on as-made heteroacenes is also demonstrated.

Scheme 1. Synthetic Routes of Ladder-Type BN-Embedded Heteroacenes

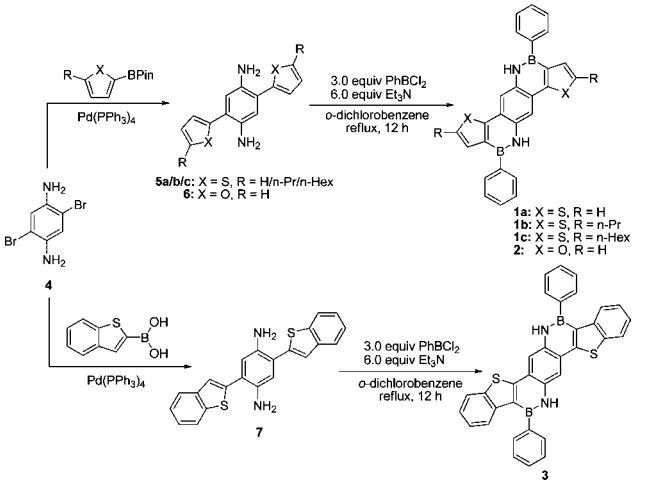

The targeted BN-embedded heteroacenes (**1**−**3**) were synthesized as depicted in Scheme 1. At first, the key intermediates of 2,5-bis-heterocycle-substituted phenylenediamines (**5a**−**c**, **6**, **7**) were prepared by Suzuki coupling of 2,5-dibromo-1,4-phenylenediamine (**4**) with the corresponding furan- or thiophene-based boronic esters. Compounds **5a**−**c** and **6** were obtained as yellow microcrystals in yields of around 60% after purification by column chromatography. Owing to the poor solubility in common organic solvents, compound **7** was obtained as a yellow powder in a low yield of ∼12% after recrystallization. Subsequently, upon treatment with an excess amount of $PhBCl_2$ (3.0 equiv) using triethylamine (6.0 equiv) as base catalyst in *o*-dichlorobenzene under refluxing conditions overnight, intermediates **5**−**7** were readily converted into the ladder-type fused heteroacenes. After final purification by silica gel column chromatography or direct precipitation from the reaction systems, compounds **1a**−**c** and **2** were obtained as yellow powders in high yields (65−85%), and compound **3** was afforded as a brown powder with a yield of 70%. The resulting heteroacenes exhibited good chemical stability even after exposure in air for several months.

All the new compounds were fully characterized by ^1H and ^{13}C NMR spectroscopy as well as by high-resolution mass spectrometry. Notably, the broad peak of the amino group located at around 3.8 ppm in the ^1H NMR spectra ($CDCl_3$) of intermediates **5b**,**c** disappeared in the spectra of target molecules **1b**,**c**. In contrast, the pronounced chemical shift of protons in the nitrogen sites appeared at about 7.9 ppm, which suggests the aromatic character of BN-fused rings. These BN-embedded heteroacenes exhibit good thermal stability with a weight loss of 5% at about 320−380 °C on the basis of thermal gravimetric analyses (Figures S1−4, Supporting Information).

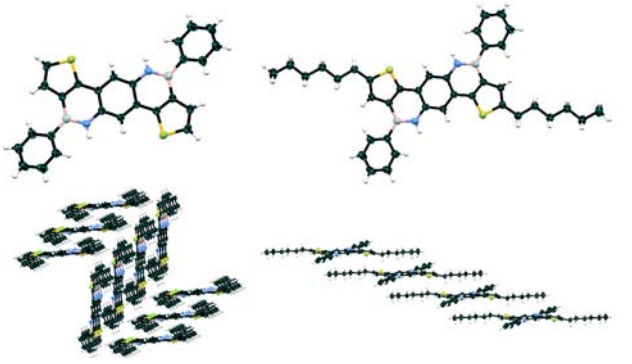

Figure 2. Crystal structures and packing diagrams for **1a** (left) and **1c** (right).

The chemical identities of compounds **1a** and **1c** were further confirmed by X-ray crystallographic analysis (Figure 2). The BN-fused heteroacenes show relatively planar structures, as demonstrated by the largest dihedral angles of 1.7° and 1.8° among the fused rings for **1a** and **1c**, respectively. The two substituted phenyl groups deviate from the plane of the azaborine rings by about 28° for **1a** and 23−27° for **1c**. The B−N bond lengths are 1.415 and 1.413 Å for **1a** and **1c**, respectively, within the range of those for other azaborines, and show distinct double-bond character.[11] The crystals of **1a** exhibit an edge-to-face herringbone-packing pattern. The alternating π-stacked columns are tilted at an angle of around 80°. In each of the

(7) Watson, M. D.; Fechtenkotter, A.; Müllen, K. *Chem. Rev.* **2001**, *101*, 1267.

(8) Bosdet, M. J. D.; Jaska, C. A.; Piers, W. E.; Sorensen, T. S.; Parvez, M. *Org. Lett.* **2007**, *9*, 1395.

(9) Baker, S. J.; Tomsho, J. W.; Benkovic, S. J. *Chem. Soc. Rev.* **2011**, *40*, 4279.

(10) (a) Campbell, P. G.; Marwitz, A. J. V.; Liu, S. Y. *Angew. Chem., Int. Ed.* **2012**, *51*, 6074. (b) Bosdet, M. J. D.; Piers, W. E. *Can. J. Chem.* **2009**, *87*, 8.

(11) (a) Liu, Z.; Marder, T. B. *Angew. Chem., Int. Ed.* **2008**, *47*, 242. (b) Hatakeyama, T.; Hashimoto, S.; Seki, S.; Nakamura, M. *J. Am. Chem. Soc.* **2011**, *133*, 18614.

π-stacked columns, the shortest distances of ~3.4 Å between the neighboring molecules manifest the significant $\pi-\pi$ stacking interactions. Compound **1c** adopts slipped stacking in a head-to-tail fashion (see Figure 2). The shortest distance between the rigid backbones in parallel neighboring molecules is 3.8 Å from the α-terminal carbon atoms of the thiophene moieties, and thus, no apparent face-to-face $\pi-\pi$ stacking interactions are observed.

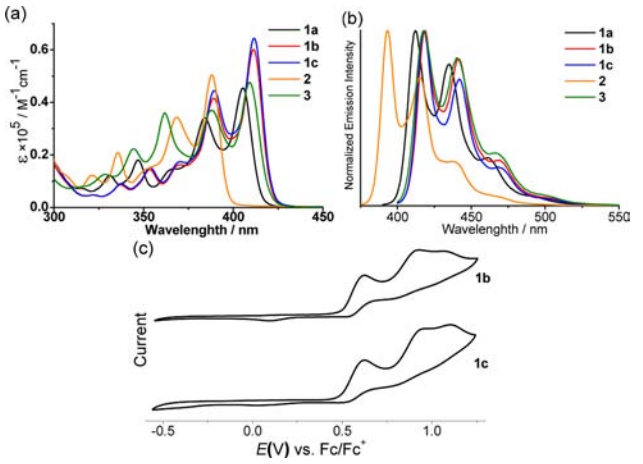

Figure 3. (a) Absorption spectra and (b) fluorescence spectra of **1**–**3** at 10^{-5} M in CH_2Cl_2. (c) Cyclic voltammograms of **1b** and **1c** measured in CH_2Cl_2 (0.1 mol/L of n-Bu_4NPF_6) at a scan rate of 100 mV/s.

Table 1. Photophysical Data for BN-Embedded Molecules

	UV–vis absorption		fluorescence	
compd	λ_{abs}[a] (nm)	log ε	λ_{em} (nm)	Φ_{PL}[b]
1a	405	4.65	412	0.17
1b	411	4.77	418	0.19
1c	412	4.80	418	0.20
2	388	4.69	393	0.26
3	409	4.67	418	0.27

[a] In CH_2Cl_2 (10^{-5} M). Only the longest λ_{max} are given. [b] Absolute value.

The absorption spectra of as-prepared BN-embedded heteroacenes are presented in Figure 3a, and feature vibronically split bands, indicative of their rigid conjugated structures, in line with the crystallographic analyses. The absorption maximum (λ_{max} = 388 nm) of furan-ring fused compound **2** exhibits a blue shift of at least 14 nm compared with other thiophene-ring fused analogs (Table 1), commonly attributed to their difference in electron delocalization.[12] As a consequence of the terminal modification of thiophene-ring moieties, compounds **1b**, **1c**, and **3** show quite similar absorption maxima. The relatively enhanced intensity of the peaks in the high-energy regions for compound **3** coincides with the extended aromatic skeleton with the additional terminally fused benzene rings. Interestingly, compared with the resulting BN-embedded heteroacenes, the rich carbon analogues, such as anthradithiophenes (II, Figure 1), display completely different UV–vis absorption spectra profiles, with remarkably blue-shifted absorption maxima at around 304–311 nm. Thereby, the incorporation of a BN unit into an aromatic framework indeed creates a π-conjugated system with different electronic structure, while maintaining the geometric similarities of the original backbone on the basis of crystallographic analysis.[4b]

The fluorescence spectra of BN-embedded heteroacenes show good mirror images of their corresponding UV–vis profiles (Figure 3b). The key data are summarized in Table 1. Compounds **1**–**3** exhibit blue luminescence with emission maxima from 393 to 418 nm, very close to those of their all-carbon analogs. In contrast to the larger Stokes shifts (more than 100 nm) of the all-carbon analogs, the quite smaller values of 5–9 nm for the BN-embedded heteroacenes substantially reveal that there are no remarkable structural deformations upon excitation. The moderate fluorescence quantum yields of compounds **1**–**3** (from 0.17 to 0.27) are comparable to those of other reported BN-embedded heteroacenes. Notably, lower luminescent quantum yields observed for the thiophene-based compound **1a** (Φ_{PL} = 0.17) than those of the structurally similar furan-based compound **2** (Φ_{PL} = 0.26) probably can be attributed to the stronger intermolecular interactions (such as through S–S interactions) that can quench the fluorescence to a large extent.[12] In contrast, compound **3** exhibits the strongest fluorescence (Φ_{PL} = 0.27) among the four thiophene-fused molecules. This result is likely attributed to the steric hindrance caused by the terminal fused benzene rings of **3** that impede the free rotation of the periphery substituted phenyl rings into a coplanar conformation with the heteroacene backbone, which may hinder the intermolecular interaction in solution.

The electrochemical behavior of BN-embedded heteroacenes **1b** and **1c** was subsequently investigated by cyclic voltammetry (CV) in CH_2Cl_2. The CVs of **1b** and **1c** both reveal two successive irreversible oxidation processes (at 0.62 and 0.93 V, respectively) followed by unresolved shoulder peaks, which probably originated from the aggregates of the charged intermediates (Figure 3c).[13] Accordingly, the HOMO energy level of −5.42 eV was derived from the first oxidation potential (assuming Fc/Fc^+ at −4.8 eV), and the LUMO energy level (at −2.47 eV) was calculated based on the absorption edges (both at 420 nm). Owing to their poor solubilities, the CVs of other BN-embedded heteroacenes **1a, 2** and **3** were measured in THF solution (see the Supporting Information).

Next, we conducted density functional theory calculations (RB3LYP/6-31G(d) level) on the BN-embedded heteroacenes **1**–**3** (see Supporting Information). All the

(12) de Melo, J. S.; Elisei, F.; Gartner, C.; Aloisi, G. G.; Becker, R. S. *J. Phys. Chem. A* **2000**, *104*, 6907.

(13) Zhang, F.; Götz, G.; Winkler, H. D. F.; Schalley, C. A.; Bäuerle, P. *Angew. Chem., Int. Ed.* **2009**, *48*, 6632.

Table 2. EL Device Performance[a]

	V_{on} (V)	L_{max} (cd m^{-2})	η_c (cd A^{-1})	η_p (lm W^{-1})	λ_{max} (nm)	η_{ext} (%)	CIE (x,y)
I	3.8	6510	1.80	0.99	458	1.3	0.16,0.16
II	3.4	5159	2.02	1.17	496	0.9	0.17,0.39
III	3.8	6416	1.70	1.00	458	1.4	0.16,0.17
IV	3.2	5077	1.39	0.85	496	0.6	0.18,0.38

[a] Abbreviations: V_{on} , voltage required for 1 cd m^{-2}; η_c, maximum current efficiency; η_p, maximum power efficiency; η_{ext}, maximum external quantum efficiency.

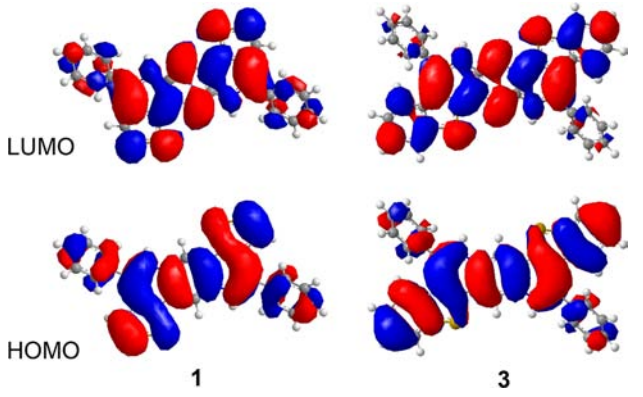

Figure 4. Calculated molecular orbitals of compounds **1** and **3**.

compounds show an almost flat backbone, with HOMOs and LUMOs of similar shapes located over the entire rigid framework, which demonstrate a fully π-conjugated system (Figure S15, Supporting Information). For instance, the steric hindrance of the terminal fused benzene rings in compound **3** leads to pendant phenyl groups deviated from the backbone plane by comparison with compound **1a** (Figure 4), which is in line with our previous fluorescence analysis. The computational HOMO energy levels of −5.37 and −5.48 eV for **1a** and **3**, are in good agreement with the values of −5.44 and −5.56 eV estimated from CVs, respectively (Table S1, Supporting Information).

Searching for organic materials with excellent blue-light emission remains an essential task for developing high-quality full-color displays and solid-state lighting applications.[14] BN-containing heteroacenes have been suggested as good blue-emitting fluorophores in some previous reports.[15] However, these molecules have not been investigated in OLEDs by far. Encouraged by the unique optical properties of BN-embedded heteroacenes for compounds **1b** and **c** described above, we fabricated OLED devices with the sandwich configuration of ITO/NPB (50 nm)/**X** = MADN:**1b** (3%) (**I**), **1b** (**II**), MADN:**1c** (3%) (**III**), **1c** (**IV**) (30 nm)/TPBI (30 nm)/LiF (1 nm)/Al (100 nm), where NPB, **X**, and Alq_3 are used as hole-transporting, light-emitting, and electron-transporting layers, respectively (see Supporting Information, Figures S16−20). The initial device performances are summarized in Table 2. When doped with only 3% MADN, the resulting devices **I** and **III** show remarkably improved color purity with increased luminescence (L_{max}) and maximum external quantum efficiencies ($\eta_{ex.}$) relative to the undoped devices **II** and **IV**. The electroluminescent performances of such blue OLED devices (η_{ext} = 1.3 for **I** and η_{ext} = 1.4 for **III**) are comparable to those of devices fabricated on the basis of heteroatom (e.g., B and S) containing π-conjugated molecules.[16]

In summary, a series of novel ladder-type BN-embedded heteroacenes were synthesized efficiently via a concise synthetic strategy, which could be multifunctionalized for diverse physical properties on account of their unique molecular skeletons. For the first time, the blue OLED devices based on BN-embedded heteroacenes were fabricated, highlighting the potential of BN-fused molecules in organic electronics.

Acknowledgment. We are grateful to Merck KGaA for financial support. We also acknowledge funding support from the Natural Science Foundation of China (NSFC 21174083), the Shanghai Committee of Science and Technology (11JC1405400), the Shanghai Pujiang Program (12PJ1405300), and Shanghai Jiao Tong University (211 Project). We thank Dr. Bin Zhang from National University of Singapore for the simulation.

Supporting Information Available. Experimental details, NMR spectra, thermogravimetric analysis, UV−vis spectra, fluorescence spectra, cyclic voltammetry, single-crystal X-ray diffraction data, and electroluminescence data. This material is available free of charge via the Internet at http://pubs.acs.org.

(14) Zhu, M.; Yang, C. *Chem. Soc. Rev.* **2013**, *42*, 4963.
(15) Lepeltier, M.; Lukoyanova, O.; Jacobson, A.; Jeeva, S.; Perepichka, D. F. *Chem. Commun.* **2010**, *46*, 7007.
(16) (a) Tsai, T. C.; Hung, W. Y.; Chi, L. C.; Wong, K. T.; Hsieh, C. C.; Chou, P. T. *Org. Electron.* **2009**, *10*, 158. (b) Noda, T.; Shirota, Y. *J. Am. Chem. Soc.* **1998**, *120*, 9714.

The authors declare no competing financial interest.